



1 **Deformation characteristics and exploratory data analysis of rainfall-induced**
2 **rotational landslide: A case study of the Zhutoushan landslide in Nanjing,**
3 **China**

4 Weiguo Li^{1,2}, Yali Liu², Libing Yang², Yanhong Chen²

5 ¹ Department of Geoinformatics, VŠB – Technical University of Ostrava, 708 00, Ostrava, Czech Republic

6 ² College of Land Science and Planning, Hebei GEO University, China

7
8 **Abstract-** Due to the complex geological structure of landslides, the installation of a monitoring network could be useful for a variety
9 of scopes studying the possible evolution of a landslide for early warning, and the occurrence of disasters of different types landslides is
10 different not only in the form of deformation, but also in the trigger factor. In the process of landslide monitoring, due to equipment
11 failure and external factors, data loss or abnormal are inevitable. In this paper, through the processing and analysis of the monitoring
12 data of the Zhutoushan landslide, the landslide is rotational landslide which is caused by the rainfall. The box plot is used to detect
13 outliers, and the polynomial fitting function and the moving average denoise method are compared to repair the data, and the latter is
14 better. Through the exploratory analysis of GNSS data, the correlation between monitoring points at different locations is found, which
15 provides a basis for the identification of landslide types.

16
17 **Keyword:** rotational landslide, trigger factor, exploratory data analysis

18 **1. Introduction**

19 Landslide is a kind of common geological hazard, which occurs all over the world and seriously threatens the safety
20 of life and property (Calcaterra et al., 2012; Yen-Yu et al., 2019; Mustafa et al., 2015), rainfall is a recognized trigger
21 (Monsieurs et al., 2019. Sidle and Bogaard, 2016). Many authors have carried out relevant studies and proposed
22 rainfall threshold and established corresponding models to predict the occurrence of landslides (Bappaditya et al.,
23 2019; Elise et al., 2019), and have developed the territorial early warning systems for rainfall induced landslide (Luca
24 et al., 2018). Some authors have also suggested that rainfall information is not sufficient to predict the occurrence of
25 landslides because it does not reflect soil moisture conditions (Koizumi et al., 2019). Only one monitoring method is
26 not enough to accurately monitor the landslide deformation. Currently, there are hydrological monitoring, geological
27 monitoring and surface monitoring. It is reasonable to set alarm thresholds for multiple parameters (Pecoraro et al.,
28 2019). However, for some landslides, the rainfall will cause changes in other monitoring parameters.

29 For the landslide early warning system, the method of mathematical model is often used to predict, and good results
30 have been achieved (Fasheng et al., 2018; Xing et al., 2018). However, the precondition of establishing mathematical
31 model is to ensure the integrity and validity of monitoring data. In the process of landslide monitoring, the loss or
32 abnormality of monitoring data caused by monitoring equipment failure or external factors is inevitable (Yong et al.,
33 2019). For abnormal data, it is necessary to know clearly whether it is caused by disturbance or equipment failure or
34 landslide deformation, so as to avoid triggering false alarm.

35 Due to the complex geological structure of landslides, the deformation of monitoring points at different locations
36 is closely related to the geological features of specific locations (Yong et al., 2019). This paper provides insight into
37 landslide type and gives the relationship between rainfall and other monitoring data through the analysis of the
38 monitoring data of the Zhutoushan landslide in China and how to judge which data is outlier through exploratory data
39 analysis.

40 **2. Study area**

41 The Zhutoushan landslide lies above the residential area of Yongning town, Pukou district, Nanjing city, Jiangshu
42 province, China. The center of area is located at 118°39'37" east longitude and 32°09'24" north latitude(Fig 1).

43



Fig 1. Location of the studied landslide site

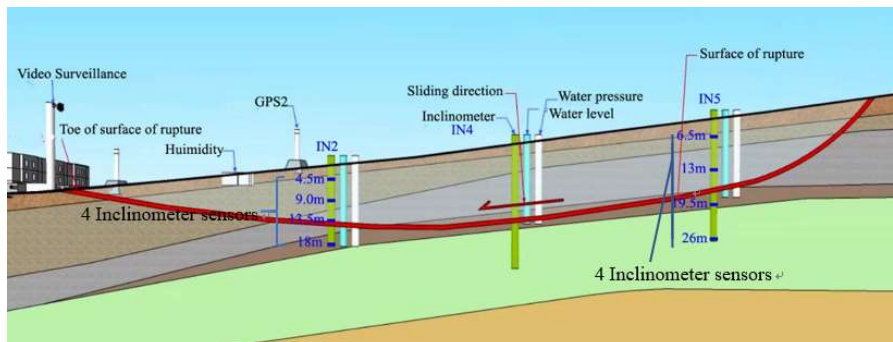
44
45
46
47
48
49
50

The working area is dissected by numerous faults linking the Zhutou mountain fault zone. The geology is composed of heavily deformed sandstone, siltstone, marlstone, limestone and soil. In the 1970s, there were large-scale mining activities at the foot of the Zhutoushan. In the process of land management, unreasonable excavation leads to many landslide disasters, and many houses are destroyed at the foot of slope, resulting in large property losses and a large number of people threatened by landslides.

51 3. Material and methodology

52 In order to monitor the deformation of zhutoushan landslide in real time, the automatic deformation monitoring and
53 warning system based on GNSS is adopted. The system integrates GNSS high-precision positioning technology,
54 wireless communication technology, database technology, General Packet Radio Service (GPRS) communication
55 technology, sensor technology and other new technology achievements, and can monitor the landslide in real time
56 and timely predict and analyze the monitoring results.

57 According to the design requirements and field investigation, This system was composed of one GNSS reference
58 station which was located outside of the landslide, eight GNSS monitoring stations (Fig 1)(the GPS8 is outside the
59 area affected by landslide deformation), six inclinometer monitoring points and each point was installed with four
60 sensors at each depth to detect slope deformation, four water level monitoring points, three pore water pressure(PWP)
61 monitoring points, one rainfall monitoring point which was installed at the edge of the landslide(Fig 2 and Fig 3),
62 one soil water content(SWC) monitoring point and two video monitoring points. The system was initiated in July
63 2017, and data were sent to the computer center in real time using the wireless sensor network technology.



64



65

Fig 2. Positions of the monitoring instruments



66

67

Fig 3. Monitoring instruments on the landslide

68

The methodology used involved: (a) GNSS data, inclinometer data, rainfall data, soil water content data and water pressure data come from the landslide early warning system, (b) data analysis using Exploring Data Analysis (EDA) method to establish the relationship between rainfall and the other data, and find outlier and characteristics of GNSS data.

69

70

71

72

4. Analysis and results

73

4.1 Rainfall and Displacement

74

In most of the cases, the main trigger of landslides is heavy or prolonged rainfall. A detailed review of the literature reveals that numerous landslides have been related to rainfall (Heyerdahl et al. 2003; Glade et al. 2000; Zezere et al. 2005). During heavy rains, water seeps into the ground and travels through unsaturated soils. This water may perch on lower permeability materials or a drainage barrier such as bedrock and highly impermeable clays.

75

76

77

78

79

80

81

82

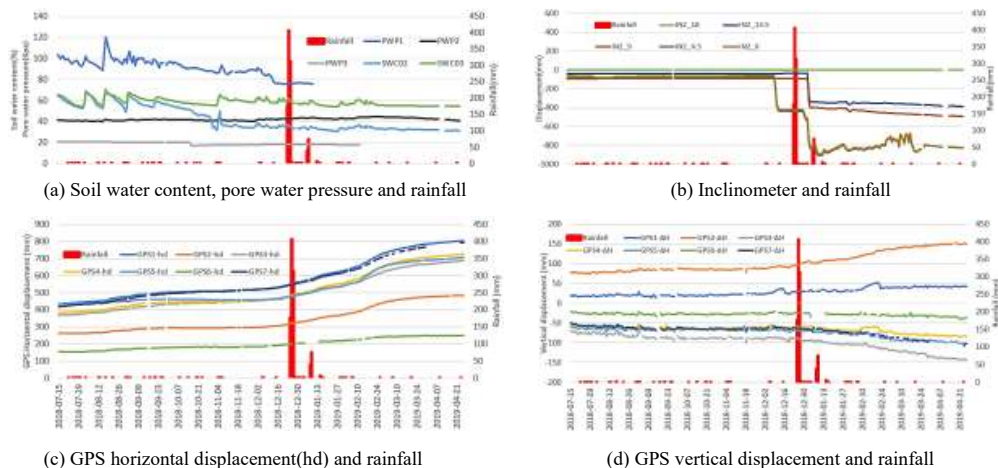
83

84

The rainfall has a great impact on the displacement of GPS surface and underground inclination. On August 15, 2018, less than 2 mm of rainfall caused changes in the horizontal displacement of the surface, but had little effect on the changes in the inclination and elevation. The rainfall over the three days of December 25, 26 and 27 in 2018 was 178mm, 406mm and 313mm, respectively. That caused dramatic changes in horizontal displacement, vertical displacement and inclination (Fig 4). The displacement of different depth for inclinometer, affected by rainfall, are also different. The deformation of the surface and buried depth of 4.5m exceeded those of the buried depth of 9m and 13.5m.

85

86



87

88

89

Fig 4. Relationship between rainfall and the other monitoring data



90 Rainfall has little effect on pore water pressure. The influence of rainfall on soil water content is also relatively
91 small, only affecting its fluctuation in a small range (Fig 4a). Even the rainfall on December 26, 2018 was 406 mm,
92 these changes are not obvious.

93 4.2 Detect outliers in raw data

94 In the process of GPS data collection and transmission, measurement error and random noise are inevitable. By
95 establishing the corresponding mathematical model or error processing, the influence of error and noise on the
96 original data can be reduced. However, for outlier, it greatly affects the quality of data and the judgment and modeling
97 of original data. Therefore, in establishing the corresponding mathematical model, it is necessary to judge the outlier
98 of the original data and remove the outliers.

99 Box plots can be used to detect outliers in raw data. GPS1 has an abnormal value in the elevation direction, and x,
100 y, and horizontal directions are normal (Fig 5). The vertical displacement of GPS1 can be fitted by a basic 20 days
101 moving average method. With this method, each observation is replaced by an average (Fig 6). But some important
102 information can be covered. Moving average denoising method is suitable (LI et al., 2016; JI et al., 2015; JI et al.,
103 2015 May). Using this method, the Root Mean Square Error (RMSE) is used to judge the outliers and replace them
104 with the average value (Fig 7). The other values are still observations. Because some important information from the
105 raw data are available.

106 For the same data, polynomial fitting model is adopted, and it is found that the correlation coefficient of the second
107 method is better than that of the first method. That is to say, the accuracy of the polynomial fitting model is improved
108 after the outliers are removed. However, there will be a problem. How to judge whether the abnormal value is caused
109 by the measurement error, or whether it is a real deformation value, and whether an alarm is required. This requires
110 comprehensive consideration of various factors to make a comprehensive judgment. Since the operation of the system,
111 outliers have been caused by equipment fault.

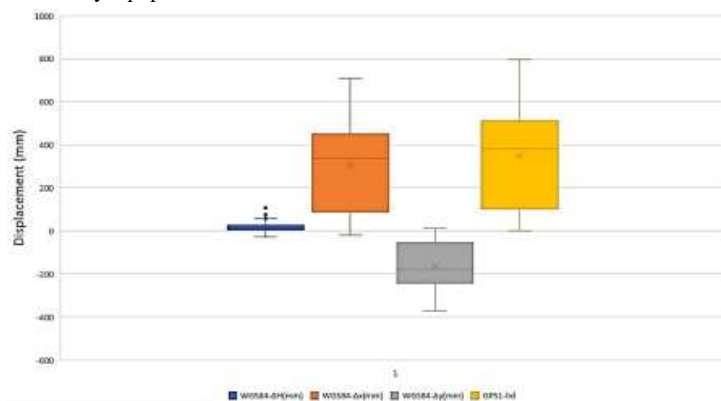
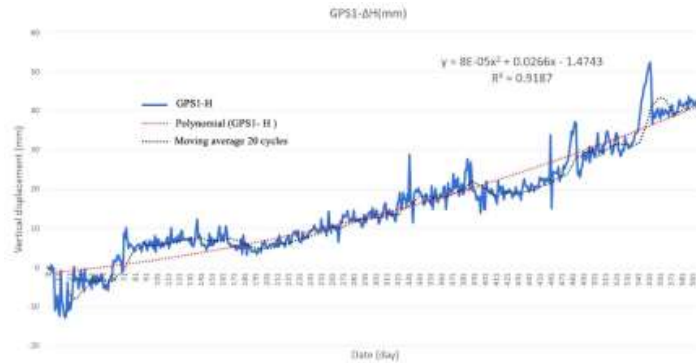


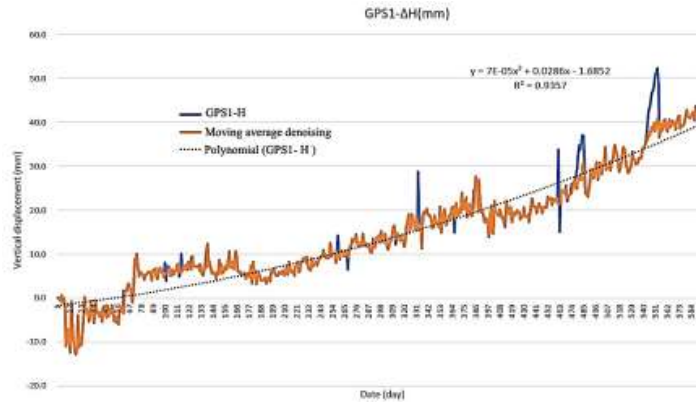
Fig 5. Box plots of GPS

112
113



114
 115

Fig 6. Vertical displacement and its fitting

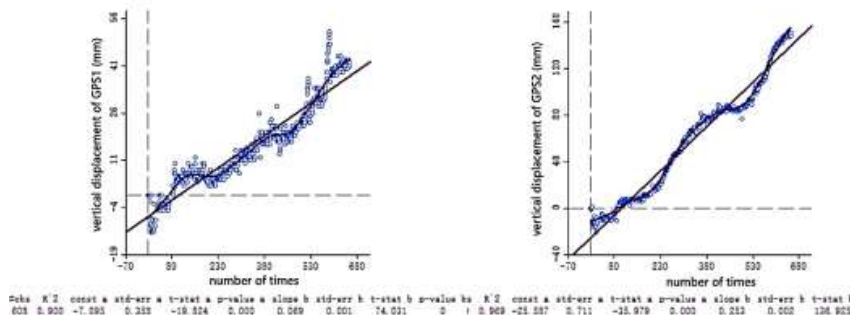


116
 117

Fig 7. Vertical displacement and its fitting

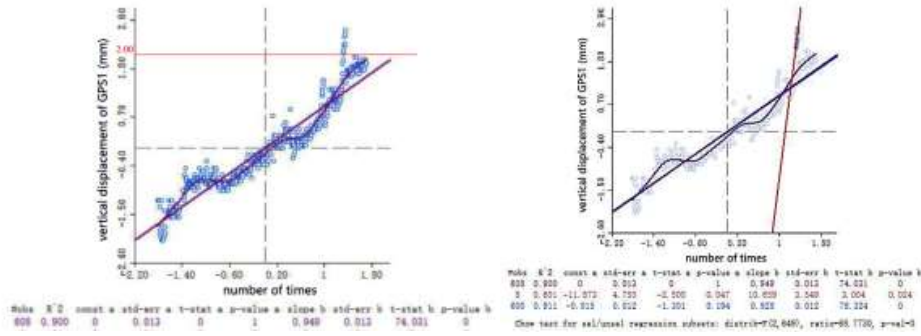
118 **4.3 Exploratory data analysis (EDA)**

119 Exploratory data analysis (EDA) is an approach to analyzing data sets to summarize their main characteristics, often
 120 with visual methods, and this method have been successfully applied to a variety of issues (Bondarev 2019).
 121 It can be seen from the scatter plots that R squared is greater than or equal to 0.9 (Fig 8 and 10). R squared of GPS3
 122 is better than the others, its value is 0.970, and R squared of GPS1 is the lowest, some points are far away from the
 123 line. The variables on both axes are rescaled to standard deviational units, so any observations beyond the value of 2
 124 can be designated as outliers (Fig 9a) (Anselin, 2005). When getting started with brushing in the scatter plot, the
 125 regression line is recalculated on the fly, reflecting the slope for the data set without the current selection (Fig 9b), R
 126 squared of GPS1 will increase to 0.911.



127
 128

Fig 8. Scatter plots of GPS1 and GPS2



(a) Standardized data of GPS1

(b) Brushing the scatter plot of GPS1

Fig 9. Analysis data of GPS1

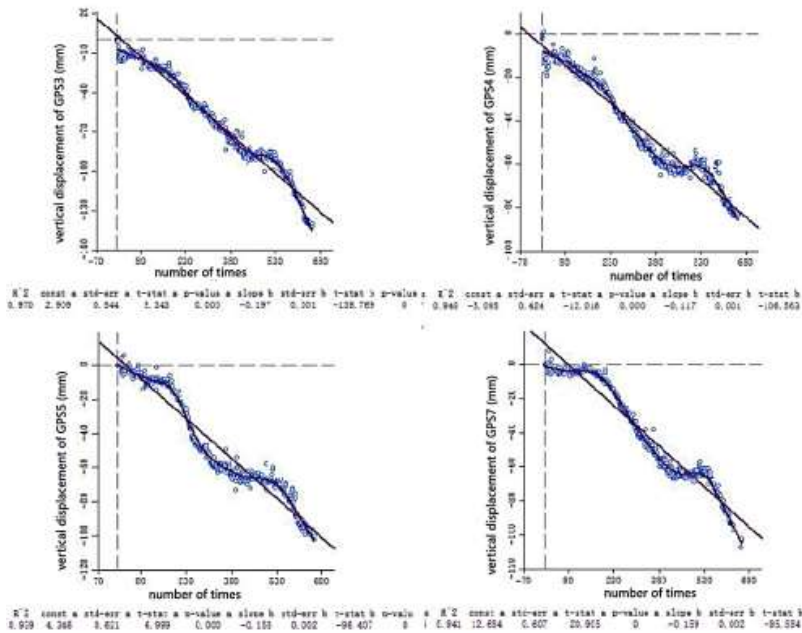


Fig 10. Scatter plots of GPS3, GPS4, GPS5 and GPS7

132
 133
 134
 135
 136
 137

Because vertical displacements of GPS1 and GPS2 are up, the others are down, the trend of vertical deformation is up or down, and the relationship between them is positive correlation. If one trend of vertical deformation is up and one trend of vertical deformation is down, their relationship is negative correlation (Fig 11).

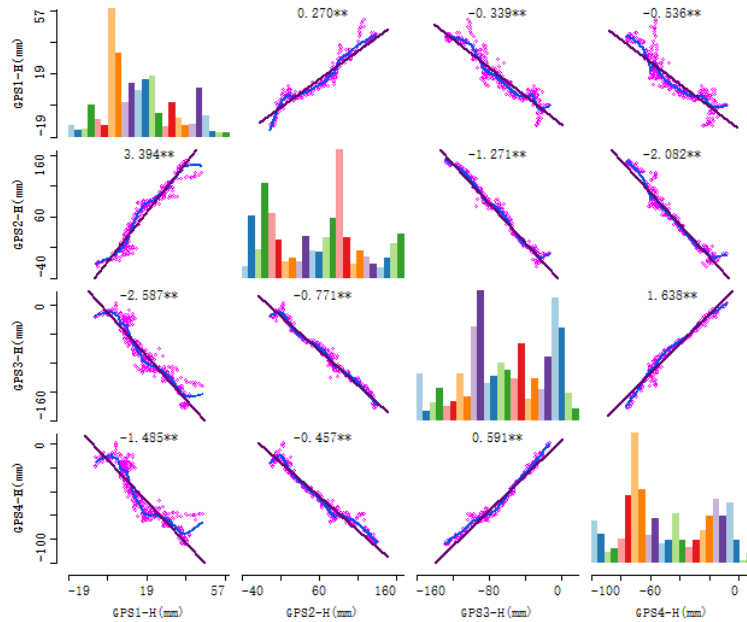


Fig 11. Scatter plot matrix between GPS1,GPS2,GPS3 and GPS4

138
 139
 140
 141
 142
 143
 144

4.4 Landslide surface displacement

The horizontal displacement direction of the eight GPS stations reflects the sliding tendency of the landslide body in the horizontal direction. It can be seen from the figure that the landslide as a whole in the direction of the northwest, and the azimuth angle is about from 310° to 330° (Fig 12). The largest horizontal displacement is GPS1, GPS8 horizontal displacement is the smallest, and the value is less than 50mm, indicating that the point is currently stable.

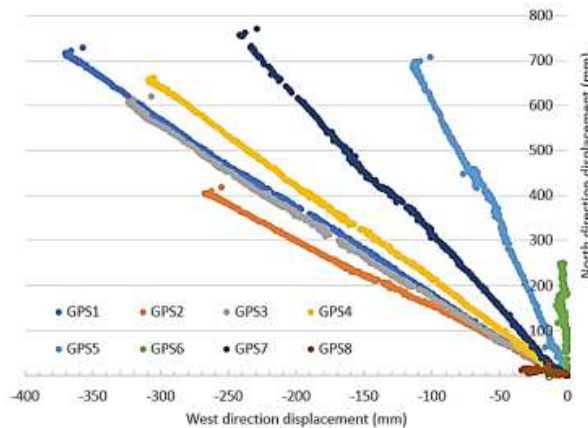


Fig 12. GPS displacement from July 14th, 2017 to May 1st, 2019

145
 146
 147
 148
 149
 150
 151

The deformation of the landslide body is not a change in one direction, but a change in three directions (Fig 13). The deformation of the north is greater than the deformation of the west, so the direction of landslide displacement is transformed into the north. The GPS1 and GPS3 monitoring points are rising in the vertical displacement, the others are opposite.

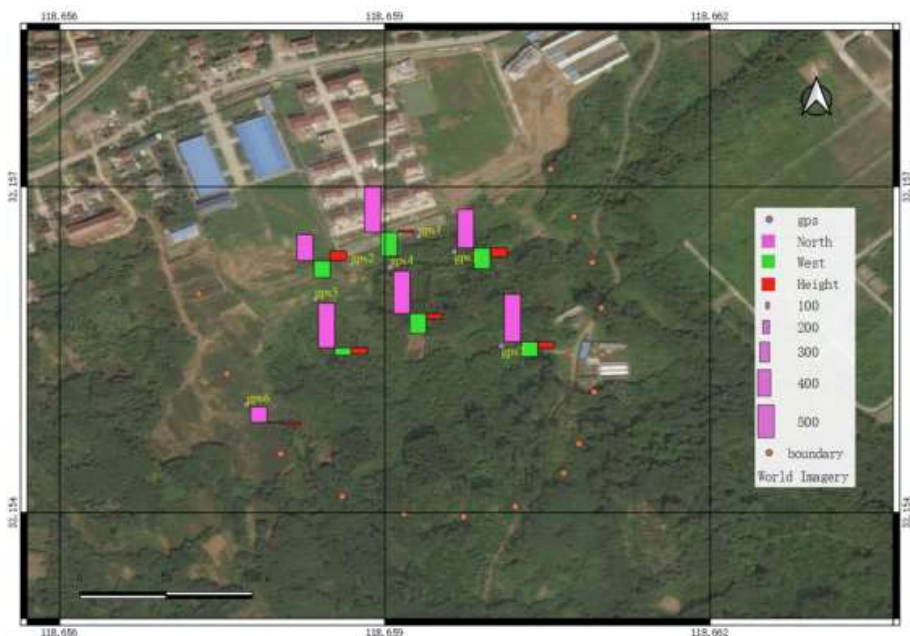


Figure 13. Surface displacement visualization (2019-04-08)

152
 153

154 The monitoring time of the Zhutoushan landslide is from July 14, 2017 to April 8, 2019. From the data analysis of
 155 GNSS monitoring points, except for GPS6 and GPS8, the vertical displacement of other points is larger (Fig 14). The
 156 horizontal displacement of the GPS1 point is the largest, reaching 792 mm. From the perspective of vertical
 157 displacement, GPS1 and GPS2 points go up, other points go down, and GPS2 and GPS3 are larger than others, the
 158 largest is GPS2 point, reaching 149.8mm. From the perspective of deformation rate, the average rate of 8 points is
 159 2mm per day, indicating that the landslide is in a stable state as a whole, but observation should be strengthened,
 160 especially for GPS1 and GPS2 at the low of the landslide. Therefore, large deformation, as time goes on, the
 161 possibility of sudden deformation of the lower part of the landslide body will increase, causing the entire landslide
 162 body to collapse.

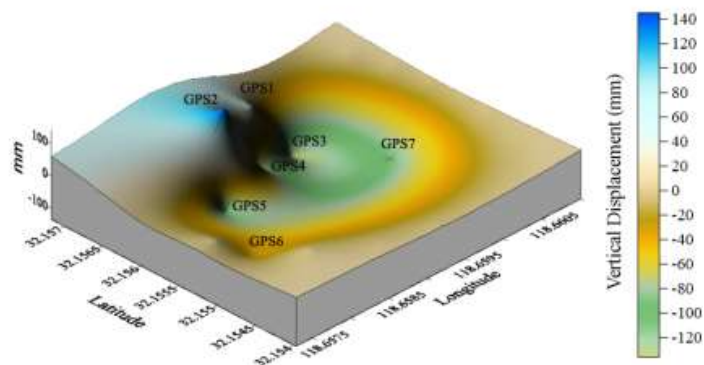


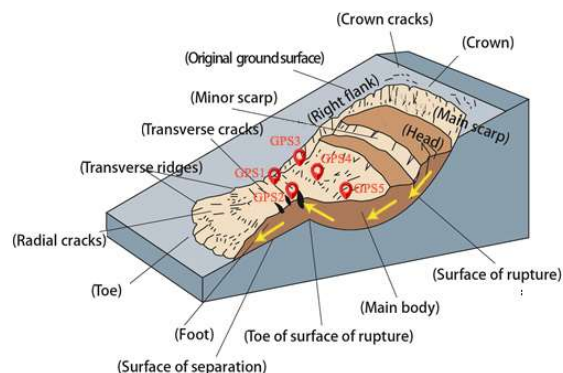
Fig 14. 3D graph on April 8th, 2019

163
 164
 165

166 5. Discussion



167 According to classification of landslides (Cruden and Varnes 1996), zhutoushan is rotational landslide (Fig 15).
168 Squeezed by the upper landslide, GPS1 and GPS2 that lie in the toe of surface of rupture rise in vertical direction.
169 Other GPS monitoring points slip down under the influence of gravity.



170

Fig 15. Zhutoushan landslide type (based on Varnes 1978)

171

172 It is very dangerous to ignore the existence of outliers in the raw data. If the outliers are included in the process of
173 data processing and analysis with exclusion, it will have a negative impact on the results. The box plots are just a
174 great tool for detecting outliers from the raw data. Polynomial fitting models and moving average noise reduction
175 methods can be used to repair outliers. From the data analysis point of view, the accuracy of the latter is better than
176 the former. The polynomial fitting model is a kind of mathematical model which can be fitted by all the raw data
177 including outliers, it will remove some important information from the raw data, and the moving average denoise
178 method will retain some. According to the setting step, the precision and retained information will also be different,
179 this requires setting the corresponding step size according to the specific project. In addition, it is necessary to
180 emphasize the judgment of the abnormal value. Whether the outlier is caused by other external factors or due to
181 landslide deformation. This requires a comprehensive judgment to avoid misjudgment and threat the people's lives
182 and damage to property. If the outliers are caused by the deformation of the landslide and exceed the deformation
183 warning value, the system should send an alarm to remind people to pay attention to safety. Otherwise, the outliers
184 can be removed from the raw data.

185 Due to the complex geological structure of the landslide, the deformation of the monitoring points at different
186 locations is related to the geological features of the landslide body and the type of landslide. Through exploratory
187 analysis of surface GNSS data, the relationship between different monitoring points is positive correlation and
188 negative correlation, which is consistent with most of the same type of landslide deformation. After standardizing the
189 data, the outliers can also be detected to improve the quality of the data.

190 6. Conclusions

191 In this paper, through the processing and analysis of the monitoring data of the Zhutoushan landslide, the landslide
192 is rotational landslide which is caused by the rainfall. The box plot is used to detect outliers, and the polynomial
193 fitting function and the moving average denoise method are compared to repair the data, and the latter is better.
194 Through the exploratory analysis of GNSS data, the correlation between monitoring points at different locations is
195 found, which provides a basis for the identification of landslide types.

196 In addition, multiple monitoring methods can be used to enhance the monitoring of the landslide, such as
197 meteorological monitoring and geological monitoring, and the mutual verification of the landslide deformation can
198 also be performed between multiple monitoring means.



199 With the development of landslide monitoring equipment, data collection, transmission and storage technology, it
200 is one of the development directions of landslide monitoring information processing in the future to mine the complex
201 relationship between massive monitoring data and various monitoring data.

202 **Software**

203 All data processing and spatial analysis were performed by QGIS 3.6.1、Surfer 15、Geoda and Matlab R2016b
204 software.

205 **Acknowledgement**

206 The authors want to thank Jianguo Kebo Space Information Technology Limited Company for kindly providing all
207 the data of the landslide. Moreover, they want to thank the reviewers for the pertinent suggestions that improved the
208 final version of the manuscript.

209 The author thank Ing. Kačmařík Michal, Ph.D. for his critical comments and suggestions, which greatly improved
210 the quality of our manuscript and map.

211 **References**

- 212 Bappaditya Koley, Anindita Nath, Subhajit Saraswati, Kaushik Bandyopadhyay² and Bidhan Chandra Ray (2019).
213 Assessment of Rainfall Thresholds for Rain-Induced Landslide Activity in North Sikkim Road Corridor in Sikkim
214 Himalaya, India. *Journal of Geography, Environment and Earth Science International* 19(3): 1-14. DOI:
215 10.9734/JGEESI/2019/v19i330086
- 216 Cruden D. M. and Varnes, D. J. (1996). ‘Landslide Types and Processes’, in A. K. Turner and R. L. Shuster (eds),
217 *Landslides: Investigation and Mitigation Transportation Research Board Special Report*, 247, pp. 36–75.
218 Washington DC: National Academy Press.
- 219 Elise Monsieurs, Olivier Dewitte, and Alain Demoulin (2019), A susceptibility-based rainfall threshold approach for
220 landslide occurrence. *Nat. Hazards Earth Syst. Sci.*, 19, 775–789. DOI:10.5194/nhess-19-775-2019
- 221 Heyerdahl H, Harbitz CB, Domaas U, Sandersen F, Tronstad K, Nowacki F, Engen A, Kjekstad O, De’voli G, Buezo
222 SG, Diaz MR, HernandezW (2003) Rainfall induced lahars in volcanic debris in Nicaragua and El Salvador:
223 practical mitigation. In: *Proceedings of international conference on fast slope movements—prediction and*
224 *prevention for risk mitigation, IC-FSM2003*. Patron Pub, Naples, pp 275–282
- 225 Fasheng Miao, Yiping Wu, Yuanhua Xie and Yaonan Li (2018). Prediction of landslide displacement with step-like
226 behavior based on multialgorithm optimization and a support vector regression model. *Landslides* (2018) 15:475–
227 488. DOI:10.1007/s10346-017-0883-y
- 228 Gaetano Pecoraro, Michele Calvello and Luca Piciullo. Monitoring strategies for local landslide early warning
229 systems. *Landslides* (2019) 16:213–231. DOI: 10.1007/s10346-018-1068-z
- 230 Glade T, Crozier MJ, Smith P (2000) Applying probability determination to refine landslide-triggering rainfall
231 thresholds using an empirical “Antecedent Daily Rainfall Model”. *Pure Appl Geophys* 157(6/8):1059–1079.
232 DOI:10.1007/s000240050017
- 233 LI Guangchun, DAI Wujiao, ZENG Fanhe (2016 Jan.). Robust Moving Average and Its Application in GPS
234 Automatic Monitoring Data Processing. *Journal of Geodesy and Geodynamics*. 2016, 36(1): 85-88.
235 DOI:10.14075/j.jgg.2016.01.019
- 236 Luc Anselin (2005 March). *Exploring Spatial Data with GeoDa™ : A Workbook*, Center for Spatially Integrated
237 Social Science. 2005 March.
- 238 Luca Piciullo, Michele Calvello, José Mauricio Cepeda (2018). Territorial early warning systems for rainfall-induced
239 landslides. *Earth-Science Reviews* 179 (2018) 228–247. <https://DOI.org/10.1016/j.earscirev.2018.02.013>
- 240 JI Lianen, ZOU Yinlong, XIN Bing (2015 Jan.). Data processing techniques on sensors of smart terminals for 3D



- 241 navigation. *Journal of Computer Application*. 2015,35(1):252-256,288. DOI:10.11772/j.issn.1001-
242 9081.2015.01.0252
- 243 JI Jiang, GAO Pengfei, JIA Nannan, YANG Rui, GUO Hanming, HU Qi, ZHUANG Songlin (2015 May). Spectral
244 Smoothing With Adaptive Multiscale Window Average. *Spectroscopy and Spectral Analysis*. 2015,35(5):1445-
245 1449. DOI:10.3964/j.issn.1000-0593(2015)05-1445-05
- 246 K Koizumi, K Oda, M Komatsu, S Ito and H Tsutsumi(2019). Slope structural health monitoring method against
247 rainfall-induced shallow landslide. *IOP Conf. Series: Materials Science and Engineering* 615 (2019) 012046.
248 DOI:10.1088/1757-899X/615/1/012046
- 249 Mustafa Zeybek, Ismail Sanlioglu, Adnan Ozdemir(2015). Monitoring landslides with geophysical and geodetic
250 observations. *Environ Earth Sci* 74:6247–6263. DOI :10.1007/s12665-015-4650-x
- 251 N. V. Bondarev (2019). Classification and Prediction of Sodium and Potassium Coronates Stability in Aqueous-
252 Organic Media by Exploratory Data Analysis Methods. *Russian Journal of General Chemistry*, 2019,89(2): 281–
253 291. DOI: 10.1134/S1070363219020191
- 254 Sidle, R. C. and Bogaard, T. A.: Dynamic earth system and ecological controls of rainfall-initiated landslides, *Earth-*
255 *Sci. Rev.*, 159,275–291, <https://DOI.org/10.1016/j.earscirev.2016.05.013>, 2016.
- 256 Stefano Calcaterra, Claudio Cesi, Caterina Di Maio, Piera Gambino, Katia Merli, Margherita Vallario, Roberto
257 Vassallo(2012). Surface displacements of two landslides evaluated by GPS and inclinometer systems: a case study
258 in Southern Apennines, Italy. *Nat Hazards* (2012) 61:257–266. DOI:10.1007/s11069-010-9633-3
- 259 Varnes DJ (1978) Slope movement types and processes. In: Schuster RL, Krizek RJ (eds) *Landslides: analyses and*
260 *control special report 176*. National Academy of Sciences, Washington, D.C., pp 11–33
- 261 Xing Zhu, Qiang Xu, Minggao Tang, Huajin Li and Fangzhou Liu (2018). A hybrid machine learning and computing
262 model for forecasting displacement of multifactor-induced landslides. *Neural Comput & Applic* (2018) 30:3825 –
263 3835. DOI: 10.1007/s00521-017-2968-x
- 264 Yen-Yu Chiu, Hung-En Chen, and Keh-Chia Yeh. Investigation of the Influence of Rainfall Runoff on Shallow
265 Landslides in Unsaturated Soil Using a Mathematical Model. *Water* 2019, 11, 1178; DOI:10.3390/w11061178
- 266 Yong Liu, Zhe Chen, BaoDan Hu, JingKun Jin, Zhao Wu(2019). A non-uniform spatiotemporal kriging interpolation
267 algorithm for landslide displacement data. *Bulletin of Engineering Geology and the Environment* (2019) 78:4153–
268 4166. <https://DOI.org/10.1007/s10064-018-1388-1>
- 269 Zezere JL, Trigo RM, Trig IF (2005) Shallow and deep landslides induced by rainfall in the Lisbon region (Portugal):
270 assessment of relationships with the North Atlantic Oscillation. *Nat Hazards Earth Syst Sci* 5:331–344. DOI:
271 10.5194/nhess-5-331-2005